

Fingerprint Matching Using Features Mapping

Gabriel B. Iwasokun, Oluwole C. Akinyokun, and Olumuyiwa J. Dehinbo

Abstract—Fingerprint systems have been featuring prominently among Biometric identification systems for individuals. The dominance of fingerprint is being promoted through continuous emergence of different forms of Automated Fingerprint Identification Systems (AFIS). In the course of performing its assigned roles, an AFIS conducts several activities including fingerprint enrolment, creation of its profile database and minutiae enhancement which involves image segmentation, normalization, Gabor filter, binarization and thinning. The activities also involve extraction of minutiae, pattern recognition and matching, error detection and correction and decision making. In this paper, a features mapping approach to fingerprint pattern recognition and matching is presented with the distance between the minutiae and core points used for determining the pattern matching scores of fingerprint images. Experiments were conducted using FVC2004 fingerprint database comprising four datasets of images of different sources and qualities. False Acceptance Rate (FAR), False Rejection Rate (FRR) and the Average Matching Time (AMT) were the statistics generated for testing and measuring the performance of the proposed algorithm. Findings from the experimental study showed the effectiveness of the algorithm in distinguishing fingerprints obtained from different sources. It is also revealed that the ability of the algorithm to match images obtained from same source is heavily dependent on the qualities of such images.

Index Terms— Features mapping, Pattern Matching, FRR, FAR, FVC2002, Fingerprint

I. INTRODUCTION

FINGERPRINT is known to be an impression of the friction ridges of all or any part of the finger. It is a deposit of minute ridges and valleys formed when a finger touches a surface. The extracted ridges and valleys from a fingerprint image are shown in Figure 1 with the ridges represented by raised and dark portions while the valleys are the white and lowered regions. A fingerprint is classified as an enrolled or latent print [1]. An enrolled fingerprint may be obtained when a person is arrested for a criminal act.

As part of the investigation process, the security agent such as a police officer will roll the arrestee's fingertip in ink before it is pressed on a card to obtain the impression. The fingerprint card is then stored in a library of such cards.

Manuscript received July 2, 2014; revised August 6, 2014. This work was supported in part by the Tshwane University of Technology, under postdoctoral fellowship programme and National Research Foundation.

Gabriel Iwasokun is with the Department of Web and Multi-Media, Tshwane University of Technology, Pretoria, South Africa (Phone: +27848435792; e-mail: IwasokunGB@tut.ac.za).

Charles Akinyokun is with Department of Computer Science, Federal University of Technology, Akure, Nigeria (Phone: +2348034059344, e-mail: akinwole2003@yahoo.co.uk).

Johnson Dehinbo is with the Department of Web and Multi-Media, Tshwane University of Technology, Pretoria, South Africa (Phone: +27822594883; e-mail: jdehinbo@yahoo.com).

Enrolled fingerprints may also be obtained with modern day fingerprint scanner [2]-[3]. The most appropriate method for rendering latent fingerprints visible, so that they can be photographed, is complex and depends, for example, on the type of surface involved.

A 'developer', usually a powder or chemical reagent, is often used to produce a high degree of visual contrast between the ridge patterns and the surface on which the fingerprint was left [1], [4].

Whether enrolled or latent fingerprint, there is an exclusive owner. This implies that no two individuals including identical twins possess same fingerprints [5]-[6]. Facts also exist that the ridges of individual finger never change throughout his or her lifetime regardless of what happens. Even in case of injury or mutilation, they reappear within a short period. The five commonest fingerprint ridge patterns are arch, tented arch, left loop, right loop and whorl with examples shown in Figure 2 [5]-[10].

In the arch patterns, the ridges enter from one side, make a rise in the center and exit generally on the opposite side. The ridges enter from either side, re-curve and pass out or tend to pass out the same side they entered in the loop pattern. In the right loop pattern, the ridges enter from the right side while the ridges enter from the left side in the left loop. In a whorl pattern, the ridges are usually circular round the core point. The core point of an image is the point of maximum or minimum ridge turning where the ridge gradient is zero.

Fingerprint has proved to be a very reliable human identification and verification index which has enjoyed superiority over all other biometrics including ear, nose, iris, voice, face, gait and signature [11]. The major reasons for these include availability for all individuals irrespective of race, gender or age and availability of easy, smooth operational and cheap fingerprint capturing devices. Other reasons include permanent form of pattern or structure over time is retained. Also, the distinct and highly unique form of individuals' features is permanently maintained.

The components of fingerprints that are mostly responsible for their high performance in identification and verification systems are categorized into three levels [3], [12]. Level One component consists of the macro details, which include friction ridge flow, pattern type, and singular points. They are mainly used for categorizing fingerprint images into major pattern types. Level Two component includes minutiae such as ridge bifurcations and endings which show significant variation from one fingerprint to another. Level Three components are the dimensional attributes of the ridge such as ridge path deviation, width, shape, pores, edge contour and other details including incipient ridges, creases, and scars. Level Two and Level Three components are mostly used for establishing fingerprints' individuality or uniqueness.

Fingerprint pattern matching is carried out when the need for ascertaining the exactness or variations among fingerprint images arises. It involves the generation of matching scores by using the level one and two components [13]. When fingerprints from the same finger are involved, the matching scores are expectedly high and low for fingerprints from different fingers.

In this study, an algorithm for fingerprint pattern matching based on minutia and core point direct distance measurement is developed. Section 2 presents the proposed algorithm for fingerprint pattern matching. The case study of the benchmark fingerprints is presented in Section 3. The findings from the case study and conclusion drawn are presented in Section 4.

II. PROPOSED FINGERPRINT PATTERN MATCHING ALGORITHM

A new method for generating fingerprints matching scores using the spatial parameters existing between the minutiae points is proposed. The motivation behind the algorithm is the need to address the matching problems due to image ridge orientation and size variations. The algorithm take advantage of the fact that the relative distance to the core point from each minutia point does not change irrespective of the image directional flow for a given image size. The core point is the point of maximum turning at which the gradient is zero. The core points are the points of maximum turning of the ridge structures in the two images. They are also the points where the directional fields experience total orientation changes [14] - [15].

Among the common feature points that uniquely describe a fingerprint image are bifurcations and ridge endings [13], [16]. Fig. 1 illustrates typical interconnecting lines between nine (9) minutiae points labeled A, B, C, D, E, F, G, H and I and the core point O in a region of an image. The connecting lines are in different directions with lengths proportionate to the distances from point O to the connecting minutiae points.

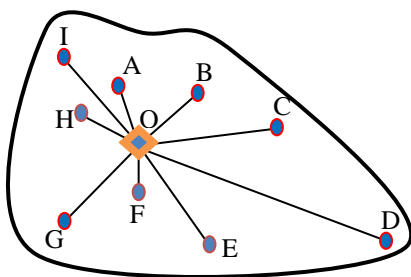


Fig 1: Interconnecting lines between feature and core points

The procedure for the proposed algorithm is in the following phases:

a. Obtain the core point using the following procedure [17]-[19]:

- The image is normalized using equation (1) where the block size is of 16×16 pixels, $M_0 = 50$ and $V_0 = 50$.

$$N(i, j) = \begin{cases} M_0 + \sqrt{\frac{V_0(I(i, j) - M_0)^2}{V_i}}, & \text{if } I(i, j) \geq M \\ M_0 - \sqrt{\frac{V_0(I(i, j) - M_0)^2}{V_i}}, & \text{Otherwise} \end{cases} \quad (1)$$

$N(i, j)$ denotes the normalized gray level value at pixel (i, j) , M_i and V_i denote the estimated mean and variance of the image I respectively.

- The local field orientation is computed as follows:

$$V_x(i, j) = \sum_{u=i-\frac{w}{2}}^{i+\frac{w}{2}} \sum_{v=j-\frac{w}{2}}^{j+\frac{w}{2}} 2\partial_x(u, v)\partial_y(u, v), \quad (2)$$

$$V_y(i, j) = \sum_{u=i-\frac{w}{2}}^{i+\frac{w}{2}} \sum_{v=j-\frac{w}{2}}^{j+\frac{w}{2}} 2\partial_x^2(u, v)\partial_y^2(u, v), \quad (3)$$

$$\theta(i, j) = \frac{1}{2} \tan^{-1} \frac{V_x(i, j)}{V_y(i, j)} \quad (4)$$

∂_x and ∂_y are the gradients in the x and y directions respectively and $V_x(i, j)$ and $V_y(i, j)$ are the local ridge orientation in the x and y directions respectively for pixel (i, j) . $\theta(i, j)$ is the least square estimate of the local ridge orientation of the block centered at pixel (i, j) . Sobel vertical and horizontal operators of size $w=3$ are used to compute ∂_x and ∂_y respectively.

- With image size of $w \times w$, the direction of gravity of the progressive blocks (non-overlapping sub-block) is defined as follows with $P = 3$:

$$A = \sum_{k=0}^{P-1} \sum_{l=0}^{P-1} V_x \quad (5)$$

$$B = \sum_{k=0}^{P-1} \sum_{l=0}^{P-1} V_y \quad (6)$$

- Fine tuning the orientation field for coarse core point detection by adjusting orientation using the following pseudo code:

Procedure:

```

    If  $f, B(i, j) \neq 0$ , then:  $\theta = 0.5 \tan^{-1} \frac{B}{A}$ 
    else:  $\theta = \frac{\pi}{2}$ 
    end
    If:  $A < 0$  then:  $\theta = \theta + \frac{\pi}{2}$ 
    If  $\theta < 0$  then
        else:  $\theta = \theta + \pi$ 
        end
    else:
        If:  $A < 0$  then:  $\theta = \frac{\pi}{2}$ 
        end
    
```

- The core point is determined upon the detection of Direction of Curvature technique by applying the following equations:

$$D_y = \sum_{k=1}^w \sin 2\theta(k, w) - \sum_{k=1}^w \sin 2\theta(k, 1) \quad (7)$$

$$D_x = \sum_{l=1}^l \cos 2\theta(w, l) - \sum_{l=1}^l \cos 2\theta(1, l) \quad (8)$$

$w=3$ is the input block size and $k=3, l=3$ are the pixel neighbourhood sizes. D_y and D_x are the difference of the directional components in y and x directions.

- The obtained core point is then used as the centre of the cropping rectangular size 100 x 100 pixels. The cropped area is defined as A_{II} .
- The orientation field is smoothed by converting to its corresponding vector field and applying a low pass filter to A_{II} .
- The optimal core point is derived from the application of Geometry of Region technique with sub-block size of 3 x 3 pixels and radius of 15 pixels.

- Obtain the x and y coordinates for all the true bifurcations and ridge endings in the thinned image. The Crossing Number (CN) value for a candidate ridge ending and bifurcation is obtained from [12], [13]:

$$CN = \sum_{i=1}^8 |N_{i+1} - N_i|, \quad N_8 = N_1 \quad (9)$$

N_1, N_2, \dots, N_8 represent the 8 neighbours of the candidate minutia point N, in its 3 x 3 neighbourhood which are scanned in clockwise direction:

Fig. 2 shows a candidate ridge pixel with CN value of 2 corresponding to a ridge ending and a CN value of 6 corresponding to a bifurcation.

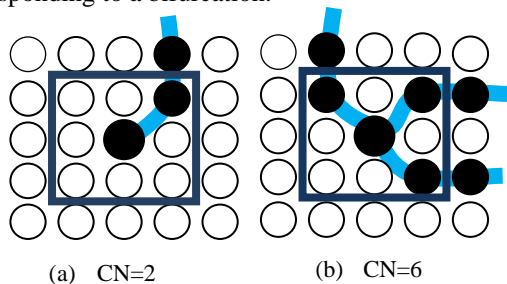


Fig 2: CN values for ridge ending and bifurcation points

For the purpose of extracting only valid minutiae from the image, a minutiae validation algorithm proposed in [13] is implemented. The algorithm tests the validity of each candidate minutia point by scanning the skeleton image and examines its local neighbourhood. An image M of size $W \times W$ centered on the candidate minutia point is firstly created before its central pixel is labeled with 2. The remaining pixels are initialised to zero.

Then for a candidate bifurcation point:

- The 3 x 3 neighbourhood of the bifurcation point is examined in a clockwise direction. The three pixels that are connected with the bifurcation point are labelled with the value of 1.
- The three ridge pixels that are linked to the three connected pixels are also labeled with 1.

- The number of transitions from 0 to 1 (T_{01}) along the border of M is counted in a clockwise direction. The candidate minutia point is validated as a true bifurcation if $T_{01} = 3$ as shown in Figure 9.

For a candidate ridge ending point:

- All the pixels in the 3 x 3 neighbourhood of the candidate point are labeled with 1.
- The number of 0 to 1 transitions (T_{01}) along the border of M is counted in a clockwise direction. The candidate minutia point is validated as a true ridge ending if $T_{01} = 1$ as shown in Fig. 3.

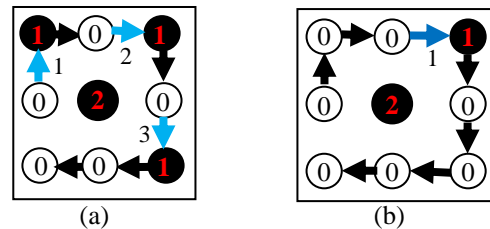


Fig. 3: 0 to 1 transitions. (a) Bifurcation ($T_{01}=3$) (b) Ridge ending ($T_{01}=1$)

- The distance, d_i between the i^{th} minutia point $P_i(r_i, s_i)$ and the image core point $M(\rho, \sigma)$ is obtained from:

$$d_i = \sqrt{(r_i - \rho)^2 + (s_i - \sigma)^2} \quad (10)$$

- The degree of closeness E_c for image K with image L is derived from:

$$E_c = \sum_{i=1}^f \frac{|G(i) - H(i)|}{G(i)} \quad (11)$$

f is the smaller of the respective number of feature points in the two images, $G(i)$ and $H(i)$ represent the distance between the i^{th} minutia point and the core points in K and L respectively.

- The correlation coefficient value, S between K and L, is then computed as the pattern matching score by using the formula:

$$S = \frac{(1 - E_c)}{100} \quad (12)$$

From this formula, the closeness value will be $E_c = 0$ for exact or same images and, consequently, the matching score will be $S = 1$.

III. EXPERIMENTAL RESULTS

The implementation of the proposed fingerprint matching algorithm was carried out using Matlab version 7.6 on Ms-Windows 7 Operating System. The experiments were performed on a Pentium 4 – 2.80 GHz processor with 1.00GB of RAM. The experiments were conducted for the analysis of the performance of the proposed algorithm when subjected to images of various qualities. The experiments also serve the basis for the generation of metric values relevant for the comparison of the obtained results with results from related works. The case study of fingerprint images obtained from Fingerprint Verification Competition was carried out. The fingerprints are in four datasets DB1, DB2, DB3 and DB4 of FVC2004 fingerprint database [20] whose summary is presented in Table I.

The database contains benchmark fingerprints jointly produced by The Biometric Systems Laboratory, Bologna, Pattern Recognition and Image Processing Laboratory, Michigan and the Biometric Test Center, San Jose, United States of America. Each of the four datasets contains 800 images that differ in qualities. The 800 fingerprints are made up of 8 images from 100 different fingers. The first two datasets were acquired using an optical fingerprint reader. The third and fourth datasets were acquired using Thermal Sweeping and computer software assistance respectively.

TABLE I:
DETAILS OF FVC2004 FINGERPRINT DATABASE

Data-base	Sensor Type	Image size	Number	Resolution
DB1	Optical Sensor	640 x 480	100 × 8	500 dpi
DB2	Optical Sensor	328 x 364	100 × 8	500 dpi
DB3	Thermal-Sweeping	300 x 480	100 × 8	512 dpi
DB4	SFinGe v3.0	288 x 384	100 × 8	About 500 dpi

False Rejection Rate (FRR), False Acceptance Rate (FAR) and Average Matching Time (AMT) were the indicators that were measured. FRR is the rate of occurrence of a scenario of two fingerprints from same finger failing to match (the matching score falling below the threshold) while FAR is the rate of occurrence of a scenario of two fingerprints from different fingers found to match (matching score exceeding the threshold). They were chosen being the commonest indicators for measuring the performance of any fingerprint pattern matching systems [3]. The FRR was measured by matching all the fingerprints from the same finger while measuring FAR was done through matching every fingerprint of each finger with all fingerprints from the other fingers. The FAR and FRR results obtained for a threshold value for the first two datasets are shown in Table II and Table III respectively.

TABLE II:
FAR AND FRR VALUES FOR DATASET DB1

Statistics	Value (%)
FAR	0
FRR	6.92

TABLE III:
FAR AND FRR VALUES FOR DATASET DB2

Statistics	Value (%)
FAR	0
FRR	8.45

These results revealed that for images obtained using optical fingerprint reader, the proposed algorithm produced FAR of 0%. The implication is that the algorithm successfully identified all the fingerprints in the two datasets that were obtained from different fingers. However, the obtained FRR values of 6.92% and 8.45% present the extent to which the algorithm failed to match fingerprints of the same finger. The FRR value of 9.07% is an indication that if the algorithm were to be used in a real-life human verification and authentication scenarios with images in Dataset DB1, 6.92 out of 100 genuine attempts will fail for the selected threshold. Similarly, 8.45 out of 100 genuine

attempts will fail based on images in dataset DB2. Some factors which include variation in pressure, rotation, translation and contact area during enrolment of the images in the datasets are responsible for these failure rates and their disparity [3]. These factors constrained images from the same finger to differ in quality, contrast and noise level. Consequently, different matching scores for different pairs of fingerprints of the same finger. The obtained FAR and FRR values obtained for the dataset DB3 are presented in Table IV. The proposed algorithm produced an FAR of 0% and an FRR of 7.63%. The algorithm also recognized fingerprint images captured from different fingers using capacitive fingerprint reader. However, FRR value of 7.63% revealed the extent to which the algorithm could not match same finger images in the dataset.

TABLE IV:
FAR AND FRR VALUES FOR DATASET DB3

Statistics	Value (%)
FAR	0
FRR	7.63

TABLE V:
FAR AND FRR VALUES FOR DATASET DB4

Statistics	Value (%)
FAR	0
FRR	9.07

Dataset DB4's FAR and FRR values are shown in Table V with values revealing that the proposed algorithm produced an FAR of 0% for images in dataset DB4 which means unique identification of fingerprints captured from different fingers using computer aids. The obtained FRR value of 9.07% indicates the degree to which the algorithm could not match images in dataset DB4 that are from the same finger. This lowest FRR value of 6.92% recorded for dataset DB1 is attributed to superior quality its images. Visual inspection of fingerprint images in the four datasets (Fig. 4) reveals that images in DB1 is best in term of clarity leading to better enhancement and extraction of predominantly true minutiae points.

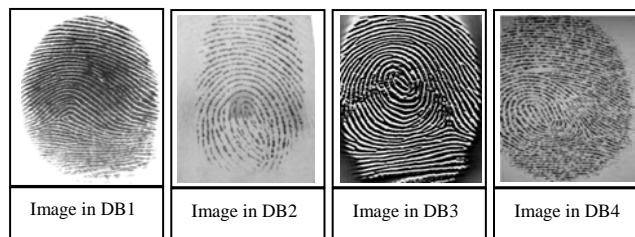


Fig. 4: Selected images from the four datasets

The highest FRR value recorded for dataset DB4 also implies that the enhancement process is more adversely affected by artifacts arising from foreign ridges and valleys introduced in form of cross over, hole or spike structures into the images during enhancement [12]-[13]. The impact of these artifacts is more pronounced as they mislead the minutiae extraction algorithms into extracting highest numbers of false minutiae (ridge ending and bifurcation) points across images from same finger thereby causing inequality in minutiae sets. The trend of the FRR values of the four datasets is represented by the straight-line graph of Fig. 5

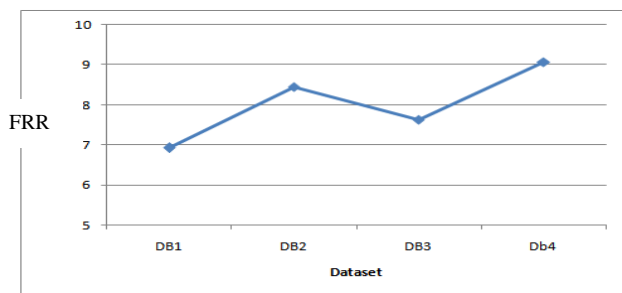


Fig. 5: The Trend of FRR values for the four Datasets

Fig. 5 shows the pattern of FRR values for the four datasets in decreasing order of 9.07, 8.45, 7.63 and 6.92 for datasets DB4, DB2, DB3 and DB1 respectively. This order is in line with the fact that dataset DB1 images are the best in terms of quality while those in dataset DB4 are the least. In the overall, the proposed pattern matching algorithm recorded average FAR of 0% and an average FRR value of 8.02% for the four datasets. The average matching times in seconds and their trend for FRR and FAR for the four datasets are presented in Table VI and the column chart of Fig. 6 respectively.

TABLE VI
 AVERAGE MATCHING TIME FOR THE FOUR DATASETS

Dataset	Average Matching time (sec)	
	FRR	FAR
DB1	0.63	0.69
DB2	0.79	0.88
DB3	0.71	0.82
DB4	0.83	0.93

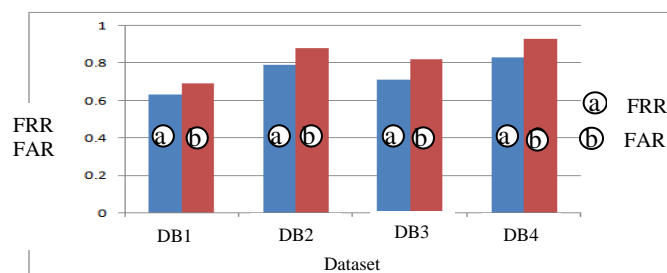


Fig. 6: Column chart of the FRR matching completion for the four datasets

Dataset DB1 has the lowest FRR average matching time of 0.63 seconds and FAR average matching time of 0.69 seconds followed by DB3, DB2 and DB4 with average FRR: FAR matching time of 0.71:0.82, 0.79:0.88 and 0.83:0.93 seconds respectively. The lowest average matching rate for dataset DB1 is attributed to fewest minutiae points and consequently, smallest number of computations. Similarly, the highest average matching times recorded for dataset DB4 indicate highest minutiae points resulting in greatest number of computations. Table VII presents obtained FRR and FAR values for four different algorithms.

The algorithms presented in [21] – [23] were selected for comparison because they are among the most recent. In Table VII, the original values obtained by the authors in [21] – [22] are presented.

However, we implemented the algorithm proposed in [23] under the conditions of experiments in this research to obtain the stated values.

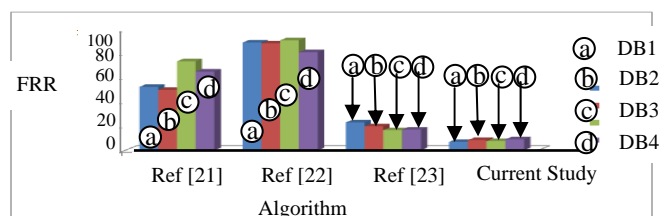


Fig 7: Colum Chart of FRR values for different fingerprint matching algorithms

TABLE VII
 FAR AND FRR FOR DIFFERENT ALGORITHMS

Data	Perez-Diaz, et al., 2010, (Ref. [21])		(Peer, 2010) Ref. [22]		(Li et a., 2009) Ref. [23]		Current Study	
	FRR	FAR	FRR	FAR	FRR	FAR	FRR	FAR
DB1	52.58	0	89.3	1.7	23.07	0	6.92	0
DB2	50.03	0	88.6	3.7	19.91	0	8.45	0
DB3	73.75	0	91.2	2.4	16.68	0	7.63	0
DB4	65.24	.015	81.3	0.9	17.09	0.01	9.07	0

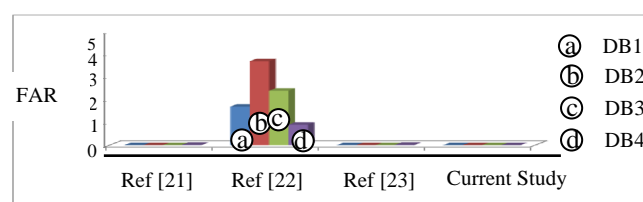


Fig.. 8: Colum Chart of FAR values for different fingerprint matching algorithms

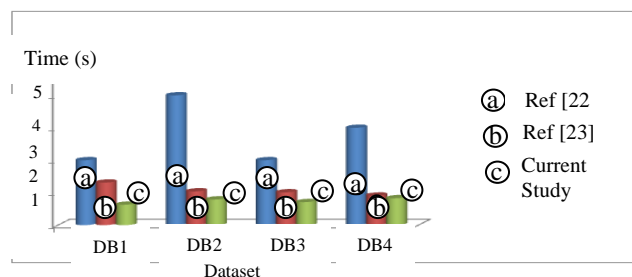


Fig. 9: Colum Chart of Computation time for FRR values for different fingerprint matching algorithms

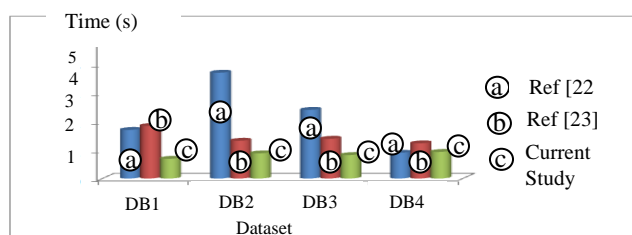


Fig. 10: Colum Chart of Computation time for FAR values for different fingerprint matching algorithms

The superior performance of the proposed algorithm over the other algorithms is clearly exhibited with its lowest FRR values for all the datasets. In addition, it is the only algorithm with an FAR value of zero for all the datasets. The column charts of Figures 7 and 8 are based on values presented in Table VII. Table VIII features the recorded computation times (in seconds) for FRR and FAR experiments in [22] – [23] and the current study.

We also implemented the original algorithm proposed in [23] under equal condition of experiments of the research to obtain the stated values. For all the datasets, the proposed algorithm has the lowest computation time, which confirms its greatest speed. Graphical representations of these values are presented in the column charts of Figures 9 and 10.

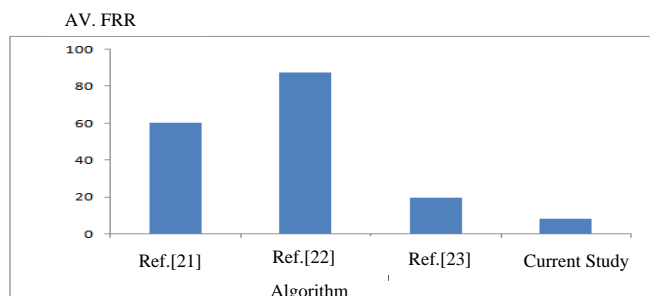


Fig. 11: Colum Chart of Average FRR values for different fingerprint matching algorithms over the four datasets

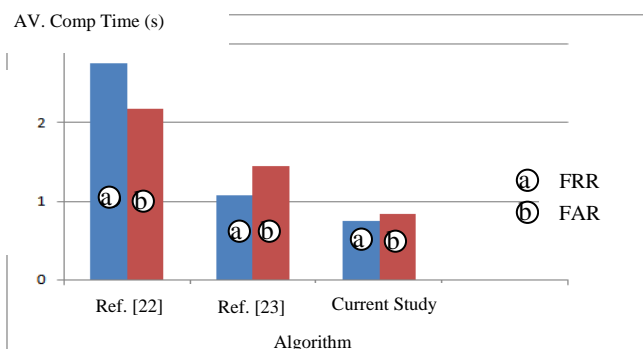


Fig. 12: Colum Chart of Average Computation time for FRR and FAR values for different fingerprint matching algorithms over the four datasets

TABLE VIII
MATCHING TIME IN SECONDS FOR DIFFERENT ALGORITHMS

Data	(Peer, 2010) (Ref. [29])		(Li et al., 2009) (Ref. [30])		Current Study	
	FRR	FAR	FRR	FAR	FRR	FAR
DB1	2	1.7	1.31	1.84	0.63	0.69
DB2	4	3.7	1.04	1.32	0.79	0.88
DB3	2	2.4	1.01	1.39	0.71	0.82
DB4	3	0.9	0.91	1.23	0.83	0.93

Fig. 11 shows the column chart of the average FRR based on the data presented in Tables VII over the four datasets while Fig. 12 represents the column chart of the average FRR and FAR computation times based on data presented in Table VIII. Visual inspection of the two Figures reveals superior performance of the proposed algorithm having recorded the least heights in both cases.

IV. CONCLUSION AND FUTURE WORKS

The implementation of a new fingerprint pattern matching algorithm has been presented. The algorithm used the relative distances between the minutiae and the core points. The algorithm hinged on the premise that irrespective of image orientation, each minutia point maintains constant distance with the core point for a given image size. The results obtained showed the effectiveness of the algorithm in distinguishing fingerprints from different sources with average FAR of 0%. However, the ability to match images from same source depends on the qualities of such images. Since the corruption levels vary across the used datasets, the algorithm yielded different FRR values. The first dataset is mostly affected with FRR values of 22.23% while the third dataset is least affected with FRR value of 14.51%.

The same order of performance was recorded for the FRR and the average matching time over the datasets. A comparative review of the obtained FRR, FAR and the

computation time values with what obtained for some recently formulated algorithms over the same datasets revealed best performance for the proposed algorithm. Future research direction aims at the optimization of the proposed algorithm for further reduction in the FRR values and the computation times.

REFERENCES

- [1] S. Nanavati, M. Thieme and R. Nanavati (2002): 'Biometrics, Identifying Verification in a Networked World', John Wiley & Sons, Inc., pp. 15-40
- [2] K. J. Anil, F. Jianjiang and N. Karthik (2010): Fingerprint Matching, IEEE Computer Society, pp. 36-44
- [3] H. N. McMurray and G. Williams (2007): 'Latent Thumb Mark Visualization Using a Scanning Kelvin Probe'; Forensic Science International.
- [4] W. G. Eckert (1996): 'Introduction to Forensic Science'; New York: Elsevier
- [5] FIDIS (2006): 'Future of Identity in the Information Society', Elsevier Inc.
- [6] D. Salter (2006): 'Thumbprint – An Emerging Technology', Engineering Technology, New Mexico State University.
- [7] J. Wayman, D. Maltoni, A. Jain and D. Maio (2005): 'Biometric Systems'; Springer-Verlag London Limited
- [8] O. C. Akinyokun and E. O. Adegbeyeni (2009): 'Scientific Evaluation of the Process of Scanning and Forensic Analysis of Thumbprints on Ballot Papers', Proceedings of Academy of Legal, Ethical and Regulatory Issues, Vol. 13, Numbers 1, New Orleans
- [9] L. Yount (2007): 'Forensic Science: From Fibres to Thumbprints' Chelsea House Publisher.
- [10] C. Roberts (2005). 'Biometrics' (<http://www.ccip.govt.nz/newsroom/information-notes/2005/biometrics.pdf>)
- [11] G. B. Iwasokun, O. C. Akinyokun, B. K. Alese and O. Olabode. (2011): 'Adaptive and Faster Approach to Fingerprint Minutiae Extraction and Validation'. International Journal of Computer Science and Security, Malaysia, Volume 5 Issue 4, pp. 414-424.
- [12] G. B. Iwasokun, O. C. Akinyokun, B. K. Alese and O. Olabode (2011): 'A Modified Approach to Crossing Number and Post-Processing Algorithms for Fingerprint Minutiae Extraction and Validation'. IMS Manthan International Journal of Computer Science and Technology, Indian, Vol. 6 Issue 1, pp. 1-9
- [13] L. Hong, Y. Wau and J. Anil (2006): 'Fingerprint image enhancement: Algorithm and performance evaluation'; Pattern Recognition and Image Processing Laboratory, Department of Computer Science, Michigan State University, pp. 1-30
- [14] G. B. Iwasokun, O. C. Akinyokun, B. K. Alese and O. Olabode (2012): 'Fingerprint Image Enhancement: Segmentation to Thinning', International Journal of Advanced Computer Science and Applications (IJACSA), Indian, Vol. 3, No. 1, 2012
- [15] G. B. Iwasokun (2012): 'Development of a Hybrid Platform for the Pattern Recognition and Matching of Thumbprints', PhD Thesis, Department of Computer Science, Federal University of Technology, Akure, Nigeria.
- [16] J. Atipat and S. Choomchuay (2007): An algorithm for fingerprint core point detection, 1-4244-0779-6, Vol 7, Issue 2007, IEEE
- [17] J. N. Kaur and A. Kamra (2011): A Novel Method for Fingerprint Core Point Detection, International Journal of Scientific & Engineering Research, Vol. 2, Issue 4, April-2011.
- [18] A. M. Usman, A. Tariq and S. A.. Khan (2008), "Fingerprint image: pre- and post- processing", International Journal on Biometrics, Volume 1.
- [19] D. Maio, D. Maltoni, C. R. Wayman. and A. K. Jain, "FVC2002: Second Fingerprint Verification Competition," in 16th International Conference on Pattern Recognition, 2002, 2002, pp. 811 - 814.
- [20] A. J. Perez-Diaz. and I. C. Arronte-Lopez (2010): Fingerprint Matching and Non-Matching Analysis for Different Tolerance Rotation Degrees in Commercial Matching Algorithms, Journal of Applied Research and Technology, Vol. 8, No. 2, pp. 186-199
- [21] P. Peer (2010): 'Fingerprint-Based Verification System A Research Prototype', IWSSIP 2010 - 17th International Conference on Systems, Signals and Image Processing, pp. 150-153
- [22] T. Li, C. Liang and K. Sei-ichiro (2009): 'Fingerprint Matching Using Dual Hilbert Scans', SITIS, pp. 553-559.